



ALMA MATER STUDIORUM
UNIVERSITÀ DI BOLOGNA

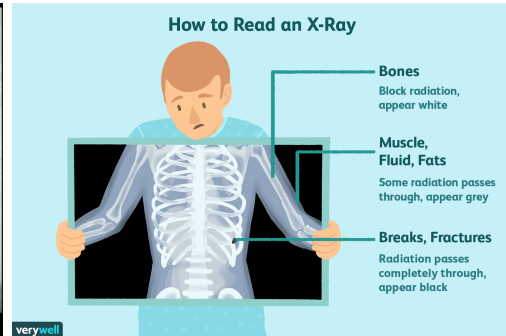
Case study: X-rays Computed Tomography (CT)

Elena Loli Piccolomini
Computational Imaging 2024-25

1. History of X-ray imaging
2. Mathematically...
3. Safer tomography
4. CT reconstruction as a linear inverse problem
5. Case study: Digital Breast Tomosynthesis

X-ray imaging

- X-rays were discovered in 1895 by the German scientist Wilhelm Conrad Rontgen.
- Radiography is an imaging technique using X-rays (or similar ionizing radiation) to view the internal form of an object

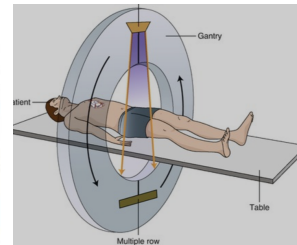
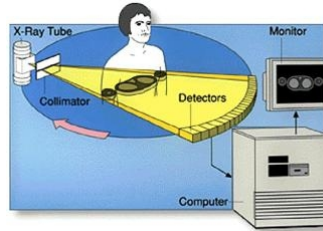


First "medical" X-ray image: hand
of Rontgen's wife, taken on 22 December 1895.

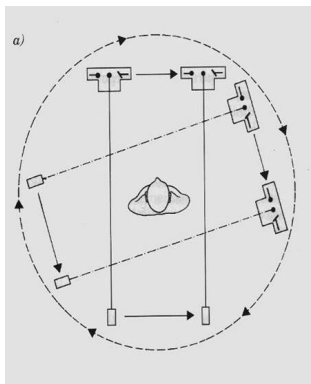
Computed Tomography

Tomography is imaging by sections:

- The word tomography is derived from Ancient Greek: tomos means "slice, section" and grapho means "to write" or "to describe".
- The circular methodology at the basis of Axial Computed Tomography (TAC) has been proposed by the English engineer Godfrey Hounsfield and by the physicist Allan Cormack, who won the Nobel prize for medicine in 1979.



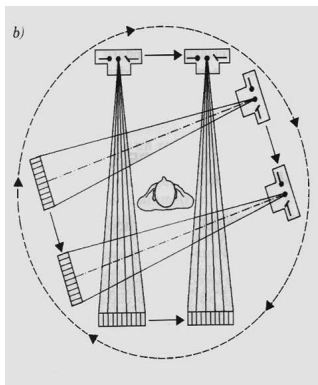
First CT generation (Hounsfield, 1971/1973)



Characteristics:

- parallel beam, one beam at a time (pencil beam)
- only one pixel in the detector
- source translation to have a complete view, then source-detector rotation (180 degrees)
- 4/5 minutes for a complete scan
- 20 minutes for a head reconstruction (slice of 13 mm)

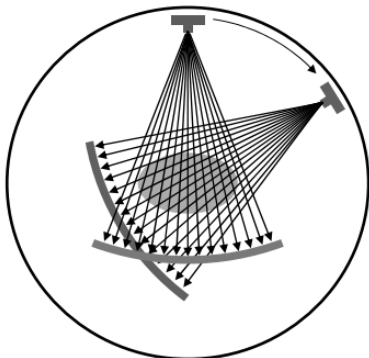
Second CT generation



Characteristics:

- each scan acquires a small range of rays (3-20 degrees), hence a larger region is visible
- the detector is constituted by more elements (3-30 pixels)
- source translation to have a complete view, then source-detector rotation (180 degrees with steps of 3-20 degrees).
- 15-30 seconds for a complete scan.

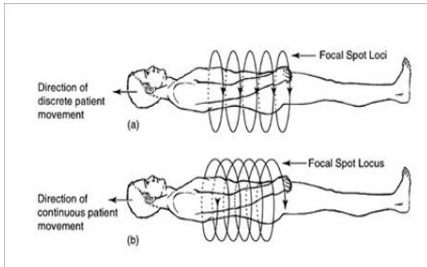
Third CT generation



Characteristics:

- Developed in 1990's
- each scan is obtained with a wide angular range (35-50 degrees), hence the whole region is visible .
- the detector is constituted by 300-800 pixels.
- the source translation is not necessary any more, hence only the source-detector rotation is performed.
- 1 seconds for a complete scan

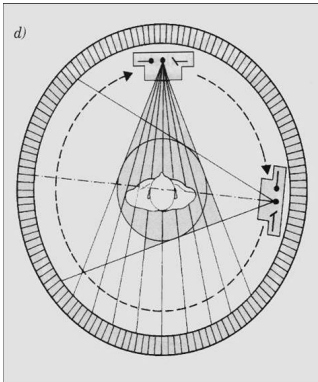
Third CT generation for volumes (multi slices)



Characteristics:

- more acquired data (on a circumference or spiral trajectory)
- a whole rotation is performed in about 1 second , hence the acquisition of a whole body requires about 40 seconds.
- They are in commerce since 1998
- with spiral multi slice (4-16 slices) about half a second for a scan.

Fourth CT generation



Characteristics:

- each scan uses a whole wide range of rays (35-50 degrees)
- the detector is fixed, with about 600-1200 pixels and encloses the patient for 360 degrees.
- only the source is rotating.
- the while scan and the reconstruction requires about 1 second.

3D medical Computed Tomography (CT) technique

In **classical** 3D CT a patient is scanned from many angular positions with high dose X-ray radiation.



<https://www.youtube.com/watch?v=7pdRq4XLT90&list=PLQpXdScJ5T8VN1c8QQCQpY5FoIJQKa0hY>

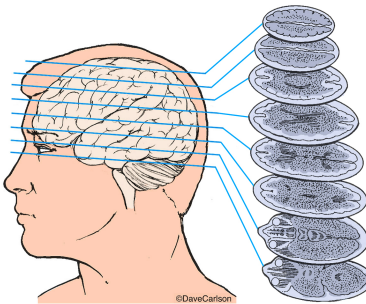
3D medical Computed Tomography (CT) technique

In **classical** 3D CT a patient is scanned from many angular positions with high dose X-ray radiation.



Features of classical 3D CT images:

- the reconstruction of a volume consists in a stack of 2D images



- it provides high quality imaging

<https://www.youtube.com/watch?v=7pdRq4XLT90&list=PLQpXdScJ5T8VN1c8QQCQpY5FoIJQKa0hY>

The sinogram

The Computed Tomography (CT) performs a (often, but not always, circular) scan: many profiles are registered, one from each angle. The set of all the acquired profiles represented in the plan (t, θ) is called **sinogram**.

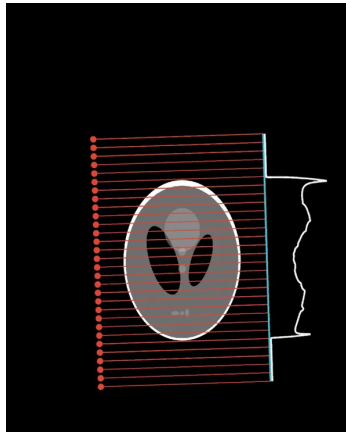
The continuous problem is modeled in terms of:

$$t \in (-\infty, +\infty) \quad \text{e} \quad \theta \in [0, 2\pi)$$

In practice, we act in a discrete setting as:

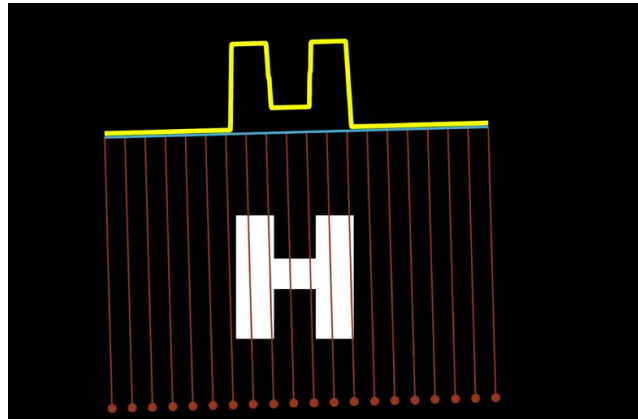
- the projections are computed from a finite number of angles $\theta_k \in \{\theta_1, \dots, \theta_{n_{angoli}}\}$;
ex:from about 300 to about 1000 angles in 180 degrees.
- the attenuation coefficients are measured only in a finite number of points t ;
 $\forall i = 1, \dots, n_{pixel}$ (where n_{pixel} is the detector resolution);
ex: detector with 600 pixel, to reconstruct an object with 512×512 voxels.
- the set $m(t_i, \theta_k) = P_{\theta_k}(t_i)$ is the sinogram.

An example



<https://www.youtube.com/watch?v=5Vyc1TzmNI8>

A further example



https://www.youtube.com/watch?v=ahyUFO_3XB4&list=PLQpXdScJ5T8VN1c8QQCQpY5FoIJQKaOhY&index=2

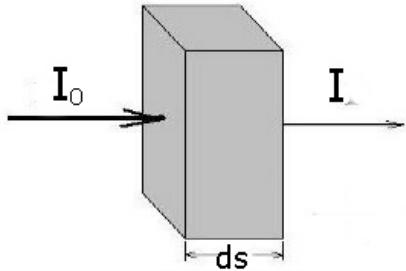
Noisy sinogram

The sinogram acquired by the detector is not exactly corresponding to the mathematical projection model due to some physical effects that we generally call *noise*.

- The first cause of noise comes from random fluctuation of the X-ray photon count from the source (shot noise or Poisson noise).
- The second cause of noise is introduced by the detector. Most X-ray CT scanners use an analog, non-photon counting detector, such as a CCD, sCMOS, or FPD. The transformation from analog to digital data produces white noise, with zero mean gaussian distribution.

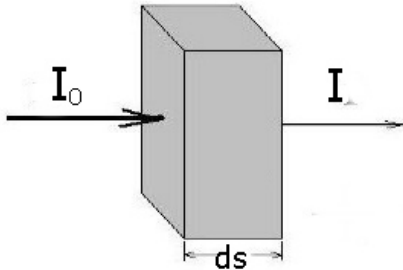
1. History of X-ray imaging
2. Mathematically...
3. Safer tomography
4. CT reconstruction as a linear inverse problem
5. Case study: Digital Breast Tomosynthesis

Single material



The X-rays source emits a single energy ray with intensity I_0 , which crosses a volume of width ds .
The detector counts I photons:
 $dI = I_0 - I$ is the number of photons absorbed by the material composing the volume.

Single material



The X-rays source emits a single energy ray with intensity I_0 , which crosses a volume of width ds .
The detector counts I photons:
 $dI = I_0 - I$ is the number of photons absorbed by the material composing the volume.

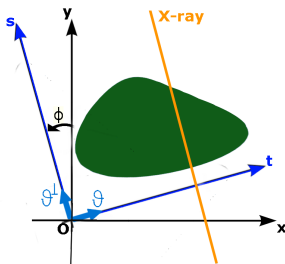
The Lambert-Beer law

$$I = I_0 e^{-\mu ds}$$

where $\mu = \mu_\lambda$ is the attenuation coefficient of the material, relative to the wavelength λ of the ray X .

The real case

Let $\mu(x, y)$ the attenuation coefficient of the X rays in the point (x, y) of the object.



We measure the intensity I of the X-ray, emitted with intensity I_0 from the source, which crossed the object along the segment L (forming an angle Φ with respect to the Cartesian axes).

It holds that:

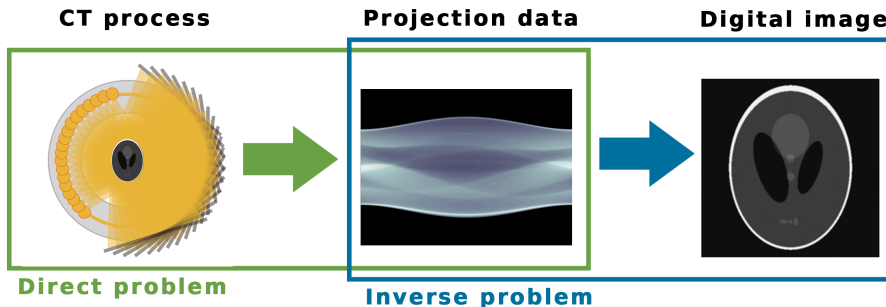
$$-\log\left(\frac{I}{I_0}\right) = + \int_L \mu(x, y) d\ell \geq 0$$

<https://www.youtube.com/watch?v=hPKpceLuSbE&list=PLQpXdScJ5T8VN1c8QQCQpY5FoIJQKaOhY&index=5>

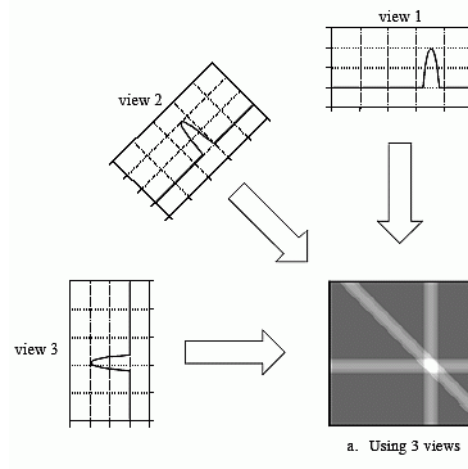
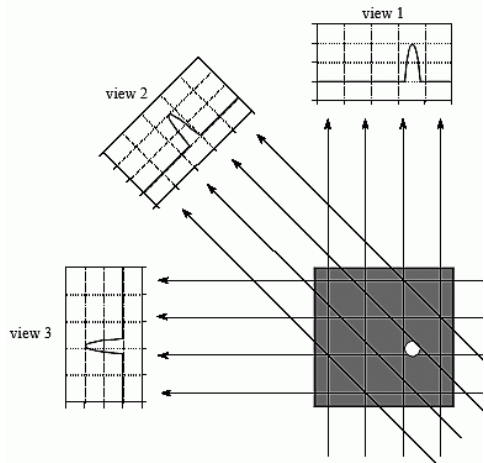
The imaging problem

The aim of CT is to compute the function $\mu(x, y)$ from the projections $m(t, \theta)$.

The reconstruction is intuitively based on the idea of *back projecting* onto the voxels of the object the values measured for each pixels of the detector at each scanning angle.



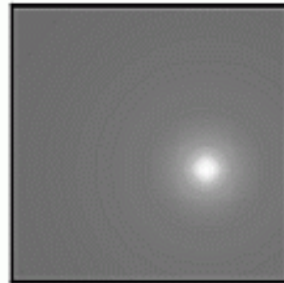
The back projection



The Back Projection

Questions:

- How to perform the back projection?
- The back projected images appear very blurred!



b. Using many views

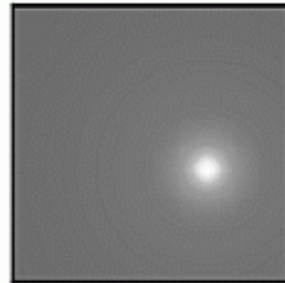
The Back Projection

Questions:

- How to perform the back projection?
- The back projected images appear very blurred!

Solution:

work in the Fourier domain on the high frequency components of the sinogram and then transform back in the image domain. In this way it is not necessary to discretize the projection integral!



b. Using many views

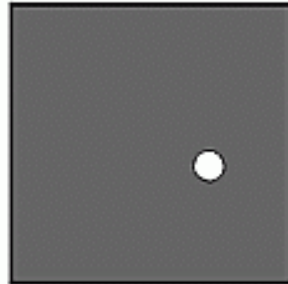
The Back Projection

Questions:

- How to perform the back projection?
- The back projected images appear very blurred!

Solution:

work in the Fourier domain on the high frequency components of the sinogram and then transform back in the image domain. In this way it is not necessary to discretize the projection integral!



b. Using many views

The Back Projection

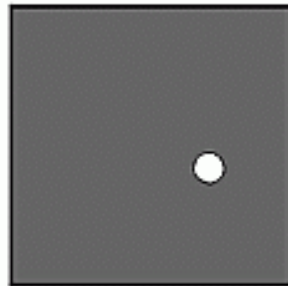
Questions:

- How to perform the back projection?
- The back projected images appear very blurred!

Solution:

work in the Fourier domain on the high frequency components of the sinogram and then transform back in the image domain. In this way it is not necessary to discretize the projection integral!

Remark: we consider a parallel beam and, initially, $\theta = 0$; hence $\mu(x, y) = \mu(t, s)$.



b. Using many views

Examples of FBP



<https://www.youtube.com/watch?v=JLFhG3ddgTU&list=PLQpXdScJ5T8VN1c8QQCQpY5FoIJQKaOhY&index=3>

1. History of X-ray imaging
2. Mathematically...
- 3. Safer tomography**
4. CT reconstruction as a linear inverse problem
5. Case study: Digital Breast Tomosynthesis

Safety in tomographic protocols

When designing CT procedures, a priority is to reduce the risks due to ionizing radiation as much as possible.

The rule is given by the **ALARA (As Low As Reasonably Achievable)** principle.

ALARA means avoiding exposure to radiation that does not have a direct benefit to you, even if the dose is small. 



Applications of safer CT

Pediatric CT



Mobile stroke unit



Dental CT

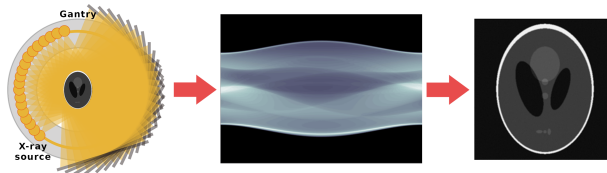


Breast Tomosynthesis



Safer tomographic protocols

Full-dose CT:

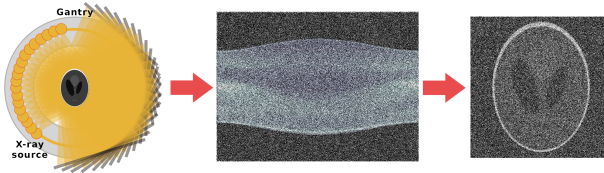


The ALARA principle is realized in two different ways, in modern CT protocols:

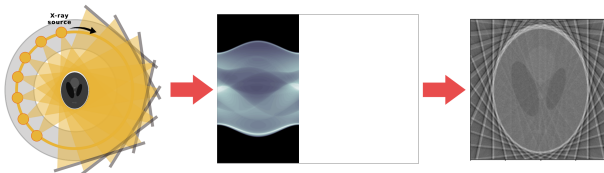
- By reducing the dose at each scan (low-dose CT) while preserving the “full” geometry (i.e., performing more than one thousand projections over the whole circular trajectory)
- By reducing the number of scans. It can be implemented by setting:
 - a large angular step between consecutive projections (sparse-view CT or few-view CT protocols)
 - a limited angular range for projections (tomosynthesis protocols).

Safer tomographies protocols

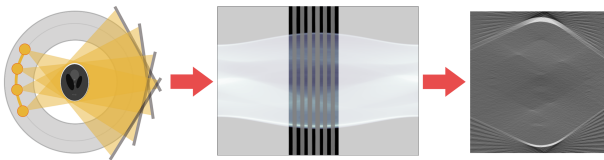
Low-dose CT:



Sparse-view CT:

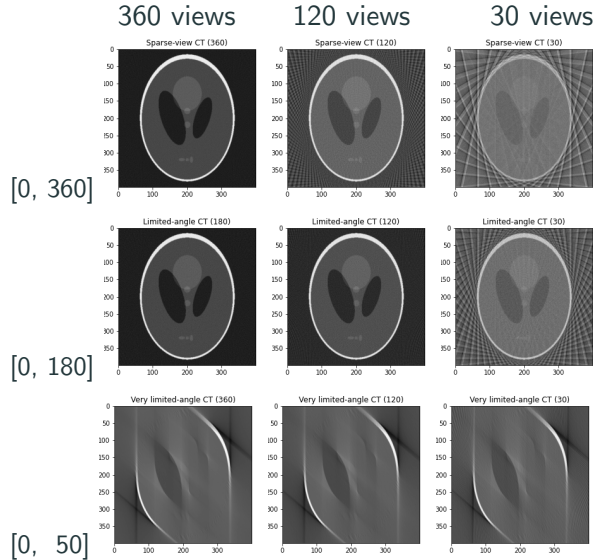
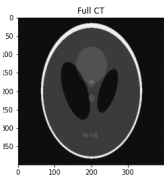


Limited-angle CT:



FBP reconstructions

FBP
reconstructions
for different
geometric
settings, of the
Shepp-Logan
phantom



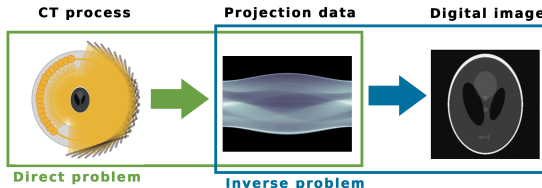
1. History of X-ray imaging
2. Mathematically...
3. Safer tomography
4. CT reconstruction as a linear inverse problem
5. Case study: Digital Breast Tomosynthesis

Tomographic inverse problem

The inverse problem of image reconstruction is **ill-posed**:

- in the case of low-dose CT, noise is amplified in the solution
- in case of sparse-view CT, infinite possible solutions exist.

Moreover, FBP-based strategies are not good solvers.

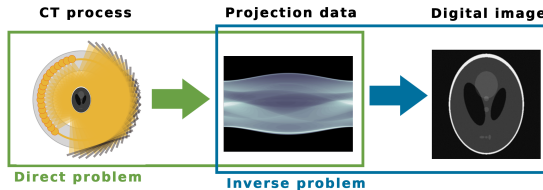


Tomographic inverse problem

The inverse problem of image reconstruction is **ill-posed**:

- in the case of low-dose CT, noise is amplified in the solution
- in case of sparse-view CT, infinite possible solutions exist.

Moreover, FBP-based strategies are not good solvers.



Hence **model-based** problem statements are used, relying on a **linear system** formulation of the imaging task. They handle prior object information and force the existence of a unique (and accurate) solution, through regularization.

CT reconstruction as a linear system (case 2D)

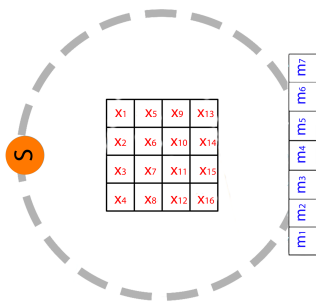


Figure 1: Scan with θ

By considering $m_i = -\log(\frac{I_i}{I_0})$, we obtain: $\sum_{j=1}^N a_{i,j} x_j = m_i$

Consider a section, of width δ mm, partitioned into a grid of $N_x \times N_y$ voxels.

Let $N = N_x \times N_y$ and x_j a single voxel, $\forall j = 1, \dots, N$ (the value $x_j \in \mathbb{R}$ corresponds to the attenuation coefficient μ of that voxel).

The Radon projection integral for a fixed angle θ is:

$$\log\left(\frac{I_i}{I_0}\right) = - \sum_{j=1}^N a_{i,j} x_j$$

where $a_{i,j}$ represents the contribution of the j -th voxel onto the i -th pixel of the detector.

CT reconstruction as a linear system

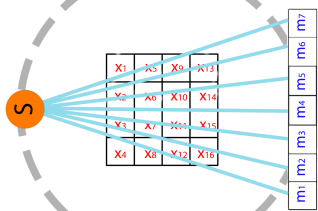


Figure 2: scan for θ_1

$$\begin{matrix} a_1^{\theta_1} \\ a_2^{\theta_1} \\ a_3^{\theta_1} \\ a_4^{\theta_1} \\ a_5^{\theta_1} \\ a_6^{\theta_1} \\ a_7^{\theta_1} \end{matrix} = \begin{matrix} x_1 \\ x_2 \\ x_3 \\ x_4 \\ x_5 \\ x_6 \\ x_7 \\ x_8 \\ x_9 \\ x_{10} \\ x_{11} \\ x_{12} \\ x_{13} \\ x_{14} \\ x_{15} \\ x_{16} \end{matrix} \times \begin{matrix} m_1^{\theta_1} \\ m_2^{\theta_1} \\ m_3^{\theta_1} \\ m_4^{\theta_1} \\ m_5^{\theta_1} \\ m_6^{\theta_1} \\ m_7^{\theta_1} \end{matrix}$$

CT reconstruction as a linear system

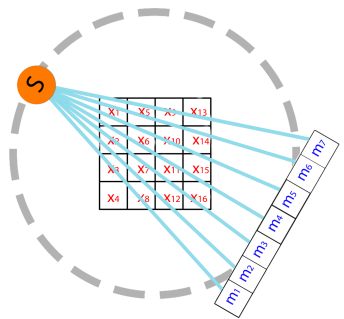


Figure 2: scan for θ_2

$$\begin{bmatrix} a_1^{\theta_1} \\ a_2^{\theta_1} \\ a_3^{\theta_1} \\ a_4^{\theta_1} \\ a_5^{\theta_1} \\ a_6^{\theta_1} \\ a_7^{\theta_1} \\ a_1^{\theta_2} \\ a_2^{\theta_2} \\ a_3^{\theta_2} \\ a_4^{\theta_2} \\ a_5^{\theta_2} \\ a_6^{\theta_2} \\ a_7^{\theta_2} \end{bmatrix} x = \begin{bmatrix} m_1^{\theta_1} \\ m_2^{\theta_1} \\ m_3^{\theta_1} \\ m_4^{\theta_1} \\ m_5^{\theta_1} \\ m_6^{\theta_1} \\ m_7^{\theta_1} \\ m_1^{\theta_2} \\ m_2^{\theta_2} \\ m_3^{\theta_2} \\ m_4^{\theta_2} \\ m_5^{\theta_2} \\ m_6^{\theta_2} \\ m_7^{\theta_2} \\ m_1^{\theta_2} \\ m_2^{\theta_2} \\ m_3^{\theta_2} \\ m_4^{\theta_2} \\ m_5^{\theta_2} \\ m_6^{\theta_2} \\ m_7^{\theta_2} \\ m_1^{\theta_2} \\ m_2^{\theta_2} \\ m_3^{\theta_2} \\ m_4^{\theta_2} \\ m_5^{\theta_2} \\ m_6^{\theta_2} \\ m_7^{\theta_2} \end{bmatrix}$$

CT reconstruction as a linear system

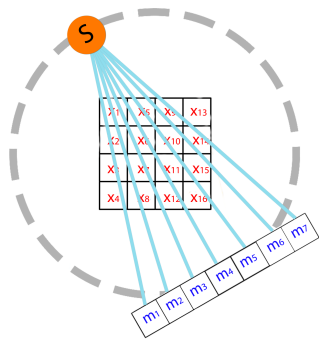


Figure 3: θ_3

$$\begin{bmatrix} A^{\theta_1} \\ A^{\theta_2} \\ A^{\theta_3} \end{bmatrix} \times \begin{bmatrix} x_1 \\ x_2 \\ x_3 \\ x_4 \\ x_5 \\ x_6 \\ x_7 \\ x_8 \\ x_9 \\ x_{10} \\ x_{11} \\ x_{12} \\ x_{13} \\ x_{14} \end{bmatrix} = \begin{bmatrix} m^{\theta_1} \\ m^{\theta_2} \\ m^{\theta_3} \end{bmatrix}$$

CT reconstruction as a linear system

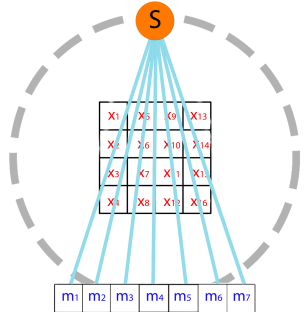


Figure 3: θ_4

$$\begin{bmatrix} A^{\theta_1} \\ A^{\theta_2} \\ A^{\theta_3} \\ A^{\theta_4} \end{bmatrix} \times \begin{bmatrix} x_1 \\ x_2 \\ x_3 \\ x_4 \\ x_5 \\ x_6 \\ x_7 \\ x_8 \\ x_9 \\ x_{10} \\ x_{11} \\ x_{12} \\ x_{13} \\ x_{14} \end{bmatrix} = \begin{bmatrix} m^{\theta_1} \\ m^{\theta_2} \\ m^{\theta_3} \\ m^{\theta_4} \end{bmatrix}$$

CT reconstruction as a linear system

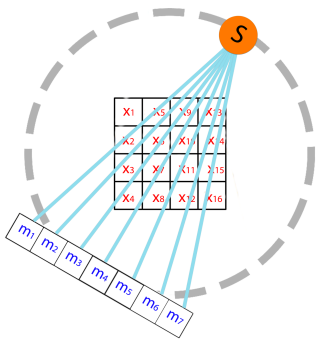


Figure 3: $\theta...$

$$\begin{bmatrix} A^{\theta_1} \\ A^{\theta_2} \\ A^{\theta_3} \\ A^{\theta_4} \\ \vdots \end{bmatrix} \times \begin{bmatrix} x_1 \\ x_2 \\ x_3 \\ x_4 \\ x_5 \\ x_6 \\ x_7 \\ x_8 \\ x_9 \\ x_{10} \\ x_{11} \\ x_{12} \\ x_{13} \\ x_{14} \end{bmatrix} = \begin{bmatrix} m^{\theta_1} \\ m^{\theta_2} \\ m^{\theta_3} \\ m^{\theta_4} \\ \vdots \end{bmatrix}$$

CT reconstruction as a linear system

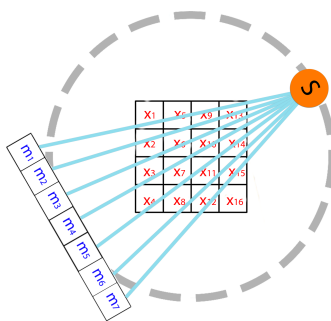


Figure 3: $\theta...$

$$\begin{bmatrix} A^{\theta_1} \\ A^{\theta_2} \\ A^{\theta_3} \\ A^{\theta_4} \\ \vdots \\ \vdots \end{bmatrix} \times \begin{bmatrix} x_1 \\ x_2 \\ x_3 \\ x_4 \\ x_5 \\ x_6 \\ x_7 \\ x_8 \\ x_9 \\ x_{10} \\ x_{11} \\ x_{12} \\ x_{13} \\ x_{14} \end{bmatrix} = \begin{bmatrix} m^{\theta_1} \\ m^{\theta_2} \\ m^{\theta_3} \\ m^{\theta_4} \\ \vdots \\ \vdots \end{bmatrix}$$

CT reconstruction as a linear system

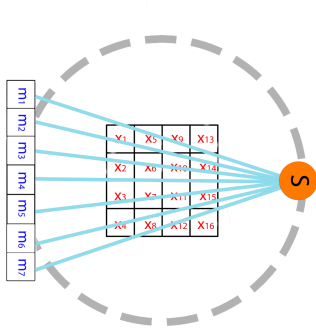


Figure 3: $\theta...$

$$\begin{bmatrix} A^{\theta_1} \\ A^{\theta_2} \\ A^{\theta_3} \\ A^{\theta_4} \\ \vdots \\ \vdots \\ \vdots \end{bmatrix} \times \begin{bmatrix} x_1 \\ x_2 \\ x_3 \\ x_4 \\ x_5 \\ x_6 \\ x_7 \\ x_8 \\ x_9 \\ x_{10} \\ x_{11} \\ x_{12} \\ x_{13} \\ x_{14} \\ x_{15} \\ x_{16} \end{bmatrix} = \begin{bmatrix} m^{\theta_1} \\ m^{\theta_2} \\ m^{\theta_3} \\ m^{\theta_4} \\ \vdots \\ \vdots \\ \vdots \end{bmatrix}$$

CT reconstruction as a linear system

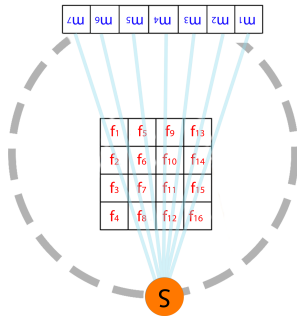


Figure 3: $\theta...$

$$\begin{bmatrix} A^{\theta_1} \\ A^{\theta_2} \\ A^{\theta_3} \\ A^{\theta_4} \\ \vdots \\ \vdots \\ \vdots \\ \vdots \end{bmatrix} \times \begin{bmatrix} x_1 \\ x_2 \\ x_3 \\ x_4 \\ x_5 \\ x_6 \\ x_7 \\ x_8 \\ x_9 \\ x_{10} \\ x_{11} \\ x_{12} \\ x_{13} \\ x_{14} \end{bmatrix} = \begin{bmatrix} m^{\theta_1} \\ m^{\theta_2} \\ m^{\theta_3} \\ m^{\theta_4} \\ \vdots \\ \vdots \\ \vdots \\ \vdots \end{bmatrix}$$

CT reconstruction as a linear system

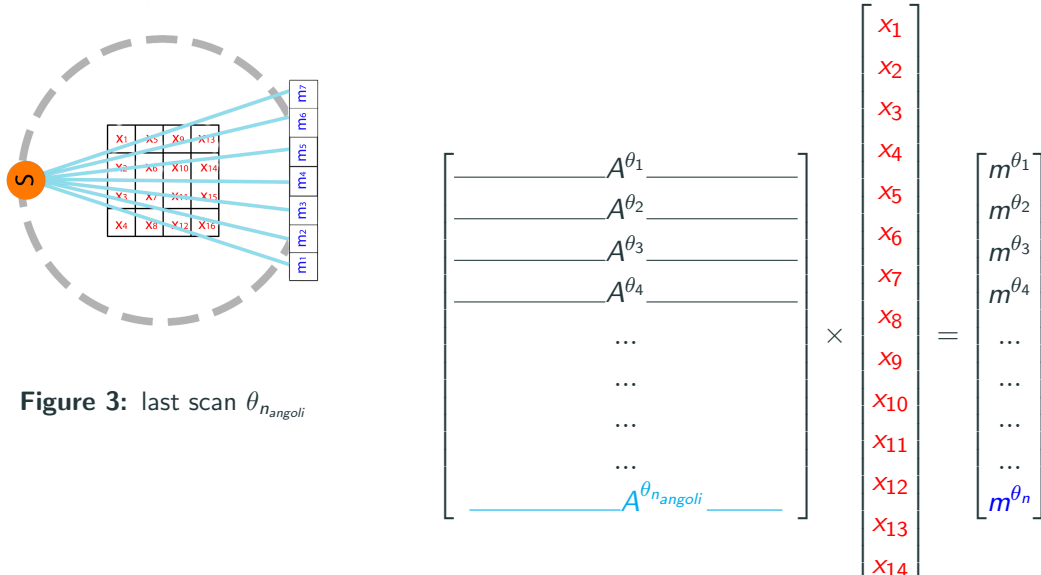


Figure 3: last scan $\theta_{n_{angoli}}$

Solving the CT linear system

The CT linear system

$$Ax = b = b_{exact} + \eta$$

con

- $x \in \mathbb{R}^{N_x N_y}$,
- $b = [m^{\theta_1}; \dots; m^{\theta_{n_{angoli}}}] \in \mathbb{R}^{n_{pixel} n_{angoli}}$,
- $A = [A^{\theta_1}; \dots; A^{\theta_{n_{angoli}}}] \in \mathbb{R}^{n_{pixel} n_{angoli} \times N_x N_y}$

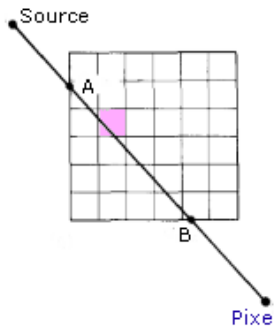
The values measured by the detector also contain the noise η due to:

- photon dispersion (scattering) and other physical effects
- inexactness of the detector counts

The noise is generally a mix of Poisson and Gauss noise.

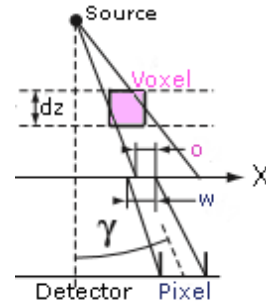
How to compute $a_{i,j}$?

Method "Ray driven"



Computes the ratio between the length of the ray intersection with voxel and the length of the ray intersection with the object.

Method "Pixel/Voxel driven"



Computes the ratio between the area of shadow the of the voxel over the pixel and the area of the pixel.

The matrix is very sparse!

A video

<https://www.youtube.com/watch?v=Uzx3uNO-nc4>

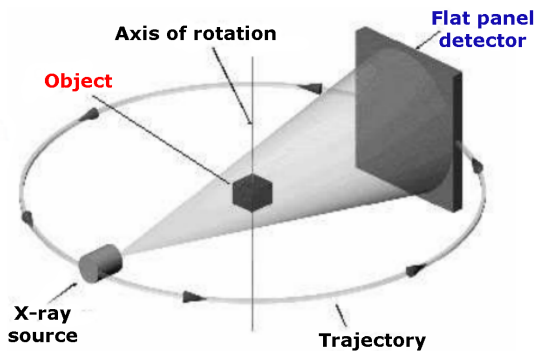
1. History of X-ray imaging
2. Mathematically...
3. Safer tomography
4. CT reconstruction as a linear inverse problem
5. Case study: Digital Breast Tomosynthesis

3D limited angle Tomography



- The object is discretized in $N_x \times N_y \times N_z$ voxels ($N_z \ll N_x$)
- The detector is discretized in $n_x \times n_y$ pixels.
- The source moves along a small circular arc (15-30 degrees)

Cone Beam Computed Tomography

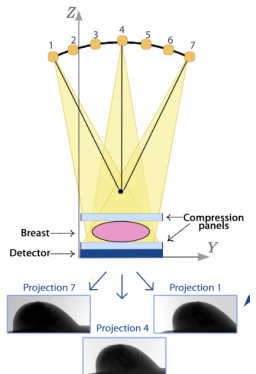


Cone Beam Computed Tomography (or CBCT, also referred to as C-arm CT, cone beam volume CT, flat panel CT or Digital Volume Tomography (DVT)) is a medical imaging technique consisting of X-ray computed tomography where the X-rays are divergent, forming a cone.

CBCT has become increasingly important in treatment planning and diagnosis in implant dentistry, ENT, orthopedics, and interventional radiology (IR), among other things.

A real case study: Digital Breast Tomosynthesis (DBT)

DBT is a recent alternative to mammography for breast screening tests, allowing for 3D breast reconstructions.



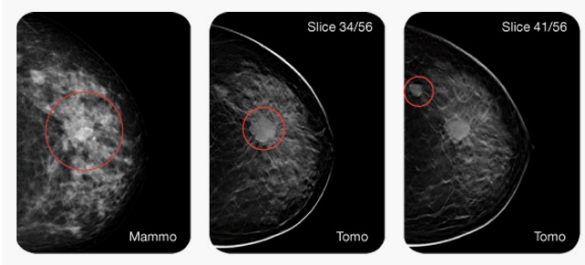
Geometric setting:

- 11/13 projections
- large angular step (3 degrees)
- soft X-rays

Software requirements:

- in-plane accuracy of 90/100 μm
- reconstructions in 45/60 seconds

Why digital breast tomosynthesis?



- DBT is a 3D emerging technique for the diagnosis of breast tumors
- It has some advantages over the traditional 2D mammography since it reduces the impact of the overlapping tissues on the tumor and makes easier the tumor detection by the radiologist.

DBT clinical applications: working with real data

Real DBT data have huge size.

An example of device setting for the a real DBT image reconstruction :

- object volume: $1168 \times 3328 \times 55$ voxels
- voxel size: $0.090 \times 0.90 \times 1 \text{ mm}$
- sinogram: $1290 \times 3190 \times 13$ pixels
- pixel size: $0.085 \times 0.85 \text{ mm}$ (on the detector)

hence

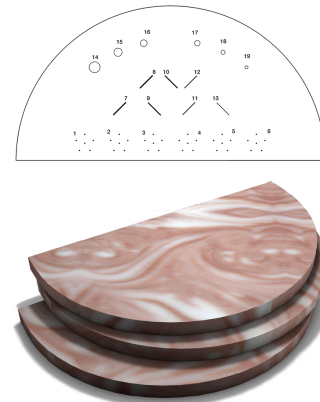
- size of the matrix A: $\approx 2.13 \cdot 10^8 \times 4.5 \cdot 10^7$
- A has $1.9 \cdot 10^{10}$ nonzero elements, meaning $\approx 320 \text{ TB}$ to store it (unfeasible!)

⇒ A must be re-computed at each A-involving step. GPU's boards are necessary to perform parallel computations.

Working with real phantoms: BR 3D¹

The "BR3D" model 020 phantom of the CIRS company.

- It is characterized by a heterogeneous background, where adipose-like and gland-like tissues are mixed in about 50/50 ratio.
- It is made of six slabs that may be arranged to create multiple anatomical backgrounds. Each slab has a semicircular shape and its size is 10 cm x 18 cm.



¹We thanks IMS (Internazionale Medico Scientifico) Giotto company for the real data sets and the collaboration.